Journal of ELECTRONIC MATERIALS
https://doi.org/10.1007/s11664-017-5957-z

$Cu_3Mo_2O_9$: An Ultralow-Firing Microwave Dielectric Ceramic with Good Temperature Stability and Chemical Compatibility with Aluminum

WANGXI WEN,[1,2] CHUNCHUN LI,[2,3,4] YIHUA SUN,[1] YING TANG,[1,2] and LIANG FANG[1,2,5]

1.—Key Laboratory of Inorganic Nonmetallic Crystalline and Energy Conversion Materials, College of Materials and Chemical Engineering, China Three Gorges University, Yichang 443002, China. 2.—Guangxi Universities Key Laboratory of Non-ferrous Metal Oxide Electronic Functional Materials and Devices, College of Material Science and Engineering, Guilin University of Technology, Guilin 541004, China. 3.—College of Information Science and Engineering, Guilin University of Technology, Guilin 541004, China. 4.—e-mail: lichunchun2003@126.com. 5.—e-mail: fanglianggl001@aliyun.com

An ultralow-firing microwave dielectric ceramic $Cu_3Mo_2O_9$ with orthorhombic structure has been fabricated via a solid-state reaction method. X-ray diffraction analysis, Rietveld refinement, Raman spectroscopy, energy-dispersive spectrometry, and scanning electron microscopy were employed to explore the phase purity, crystal structure, and microstructure. Pure and dense $Cu_3Mo_2O_9$ ceramics could be obtained in the sintering temperature range from 580°C to 680°C. The sample sintered at 660°C for 4 h exhibited the highest relative density ($\sim$ 97.2%) and best microwave dielectric properties with ε_r = 7.2, $Q \times f$ = 19,300 GHz, and τ_f = − 7.8 ppm/°C. Chemical compatibility with aluminum electrodes was also confirmed. All the results suggest that $Cu_3Mo_2O_9$ ceramic is a promising candidate for use in ultralow-temperature cofired ceramic applications.

Key words: Microwave dielectric properties, ULTCC, sintering behavior, chemical compatibility

INTRODUCTION

Nowadays, low-temperature cofired ceramic (LTCC) technology attracts wide attention due to its enormous contribution to miniaturization and cost reduction of modern wireless communication systems.[1–3] For practical applications, low-temperature cofired ceramics (LTCCs) must fulfill the requirements of appropriate relative permittivity (ε_r), high quality factor ($Q \times f$), extremely low temperature coefficient of resonant frequency (τ_f), and low sintering temperatures to enable cofiring with metal electrodes (such as Ag, Cu, and Al).[4,5] In addition, chemical compatibility, thermal conductivity, and thermal expansion are of practical interest. To date, several attempts to lower the sintering temperature of such ceramics have been made, including addition of sintering aids, soft chemical synthesis, use of nanosized particles, etc. More recently, use of glass-free low-firing ceramics has been accepted as a desirable approach for development of low-temperature cofired ceramics, because of the simple synthesis process and high dielectric performance.

In recent years, numerous low-firing ceramics have been reported, most being based on Bi_2O_3-, TeO_2-, V_2O_5-, WO_3, and MoO_3-rich systems, for example, β-$Bi_2Mo_2O_9$,[6] $MgTe_2O_5$,[7] $BaMg_2V_2O_8$,[8] Li_4WO_5,[9] and $CaMoO_4$.[10] Besides, various Cu-containing ceramics have also been reported to offer the combination of low sintering temperatures and good microwave dielectric properties[11,12]; For example, Joseph et al.[11] recently reported an ultralow-firing-

(Received April 24, 2017; accepted November 14, 2017)

Published online: 28 November 2017

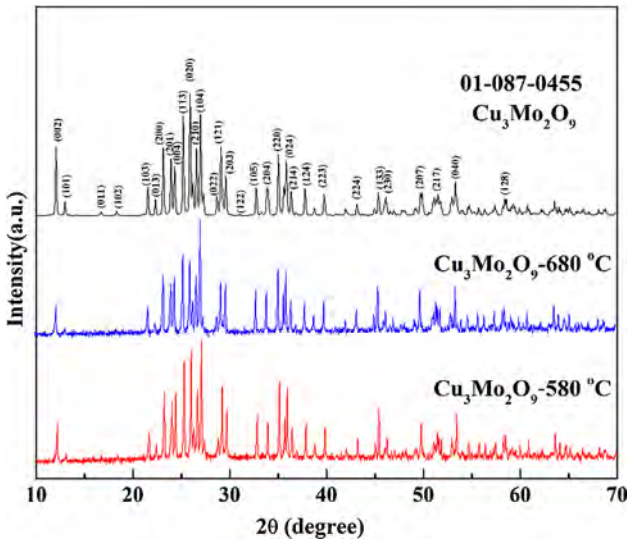

Fig. 1. XRD patterns of $Cu_3Mo_2O_9$ ceramic sintered at different temperatures.

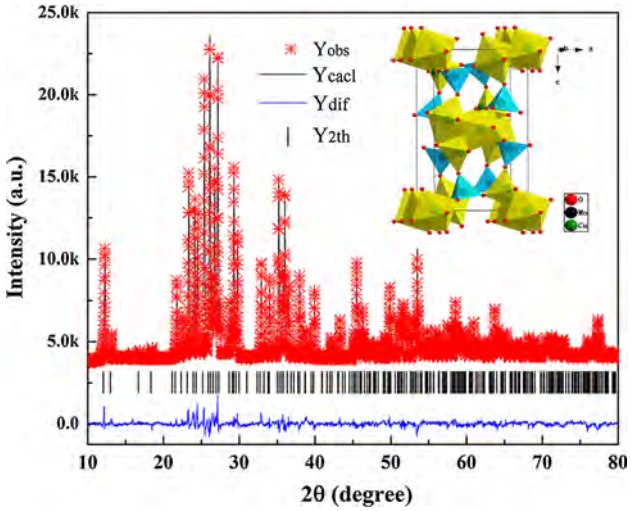

Fig. 2. Rietveld refinement patterns and crystal structure of $Cu_3Mo_2O_9$.

temperature ceramic $CuMoO_4$ with $\varepsilon_r = 7.9$, $Q \times f = 53{,}000$ GHz, and $\tau_f = -36$ ppm/°C when sintered at 650°C. In our previous work, $BiCu_2VO_6$ with ε_r of 22.7, $Q \times f$ of 11,960 GHz, and τ_f of -17.2 ppm/°C was obtained after sintering at 740°C.[12] Thus, it is reasonable to predict that a compound simultaneously containing Cu and Mo would exhibit low sintering temperature and promising microwave dielectric performance. This motivated us to search for low-temperature cofired ceramics in the CuO–MoO_3 binary system.

$Cu_3Mo_2O_9$ compound in the CuO–MoO_3 system was synthesized by Hamasaki et al.[13] in 2009, and its orthorhombic crystal structure also reported. However, to the best of the authors' knowledge, the microwave dielectric properties of $Cu_3Mo_2O_9$ ceramic have not been investigated. In this work,

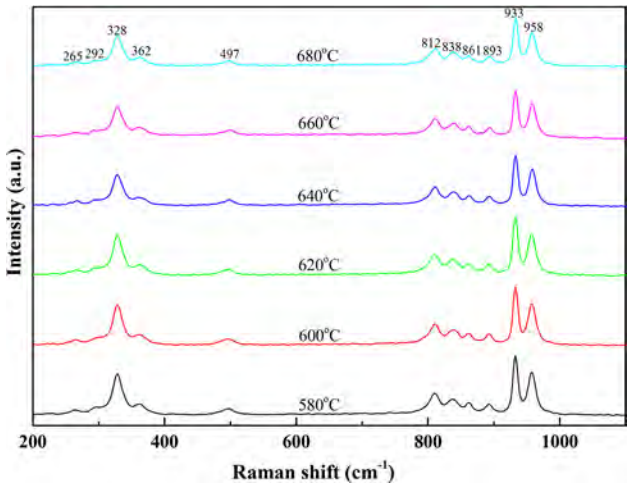

Fig. 3. Room-temperature Raman spectra of $Cu_3Mo_2O_9$ ceramic sintered at temperatures in the range from 580°C to 680°C for 4 h.

$Cu_3Mo_2O_9$ ceramic was prepared, and its sintering behavior and microwave dielectric properties studied.

EXPERIMENTAL PROCEDURES

$Cu_3Mo_2O_9$ ceramic was prepared by solid-state reaction of high-purity oxides CuO (99.99%, Guo-Yao Co. Ltd., Shanghai, China) and MoO_3 (99.99%, Guo-Yao Co. Ltd., Shanghai, China). The mixed oxides were ball-milled for 4 h using alcohol as medium. The wet mixture was dried and calcined at 580°C for 4 h, then ball-milled again for 4 h. The resulting slurries were dried and reground with poly(vinyl alcohol) (PVA) as binder. Then, the granulated powders were pressed into 10-mm-diameter 6-mm-height cylinders under uniaxial pressure of 200 MPa. The samples were first heated at 550°C for 4 h for degumming, then sintered at various temperatures (from 580°C to 680°C) in air. To evaluate the chemical compatibility of $Cu_3Mo_2O_9$ with Al electrodes, 20 wt.% Al was added to $Cu_3Mo_2O_9$ and cofired at 660°C for 4 h.

The phase composition of the sintered sample was confirmed by x-ray diffraction (XRD) analysis (X'Pert PRO, PANalytical, Almelo, The Netherlands) and Raman spectrometry (DXR; Thermo Fisher Scientific, USA). The bulk density of the specimens was measured using Archimedes' method. Scanning electron microscopy (SEM, JSM6380-LV; JEOL, Tokyo, Japan) was used to observe grain morphology. Microwave dielectric properties of the sintered ceramics were measured using a network analyzer (N5230A, Agilent Co., Palo Alto, CA) and a temperature chamber (Delta 9039; Delta Design, San Diego, CA). τ_f values were calculated using the formula

$$\tau_f = \frac{f_2 - f_1}{f_1(T_2 - T_1)}, \quad (1)$$

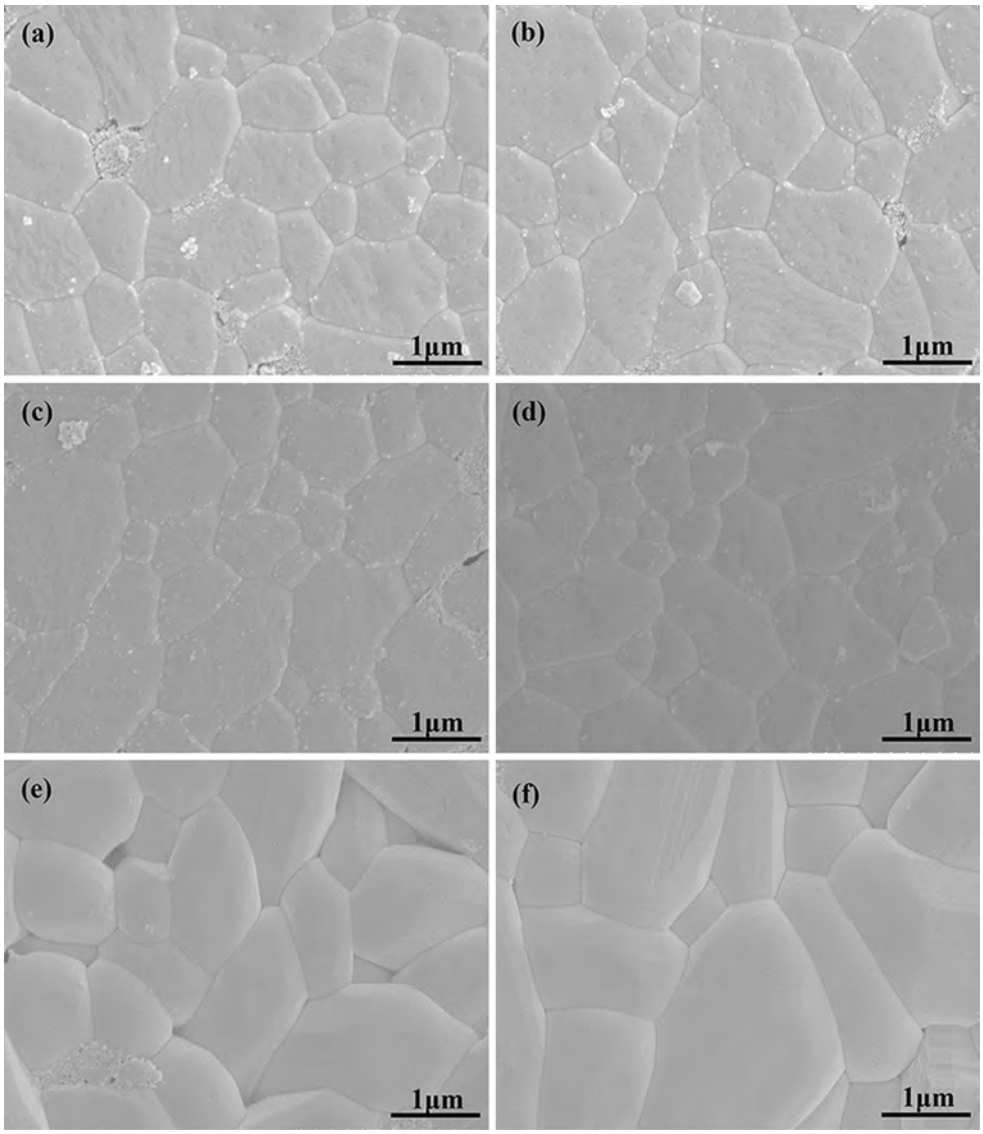

Fig. 4. SEM micrographs of $Cu_3Mo_2O_9$ ceramics sintered at temperature of (a) 580°C, (b) 600°C, (c) 620°C, (d) 640°C, (e) 660°C, and (f) 680°C.

where f_1 and f_2 represent the resonant frequency at T_1 and T_2, respectively.

RESULTS AND DISCUSSION

Figure 1 shows the room-temperature XRD patterns of $Cu_3Mo_2O_9$ samples sintered at 580°C and 680°C. The observed main peaks are consistent with the standard Joint Committee on Powder Diffraction Standards (JCPDS) file no. 01-087-0455 for $Cu_3Mo_2O_9$, without extra peaks detected. To further confirm the phase purity and exactly determine the lattice parameters, Rietveld refinement was performed based on the XRD data. As shown in Fig. 2, the good agreement between the observed and calculated XRD patterns and the low residual factors of $R_{wp} = 2.48\%$, $R_{exp} = 1.52\%$, and $R_p = 1.86\%$ suggest phase purity. The refined lattice parameters were $a = 7.6762(1)$ Å, $b = 6.8661(1)$ Å, $c = 14.6279(2)$ Å, $\alpha = \beta = \gamma = 90°$, and $V = 771$ Å^3 ($Z = 2$). The crystal structure of $Cu_3Mo_2O_9$ is shown in the inset of Fig. 2, with Cu atoms located in octahedra coordinated with six oxygen atoms while Mo atoms are bonded to four oxygen atoms to form a tetrahedron. Neighboring octahedra and tetrahedra share corners to form a three-dimensional (3D) network.

Figure 3 shows the Raman spectra of $Cu_3Mo_2O_9$ samples sintered at different temperatures (from 580°C to 680°C). The Raman spectra show 11 main peaks in the wavenumber range from 100 cm^{-1} to 1000 cm^{-1}, similar to previous reports by Moiseenko[14] and Sato et al.[15] Obviously, over the sintering temperature range, all the samples exhibited similar Raman spectra in spite of slight difference in Raman shift. Combined with the x-ray diffraction analysis, it can be concluded that single-phase $Cu_3Mo_2O_9$ in space group *Pnma* was

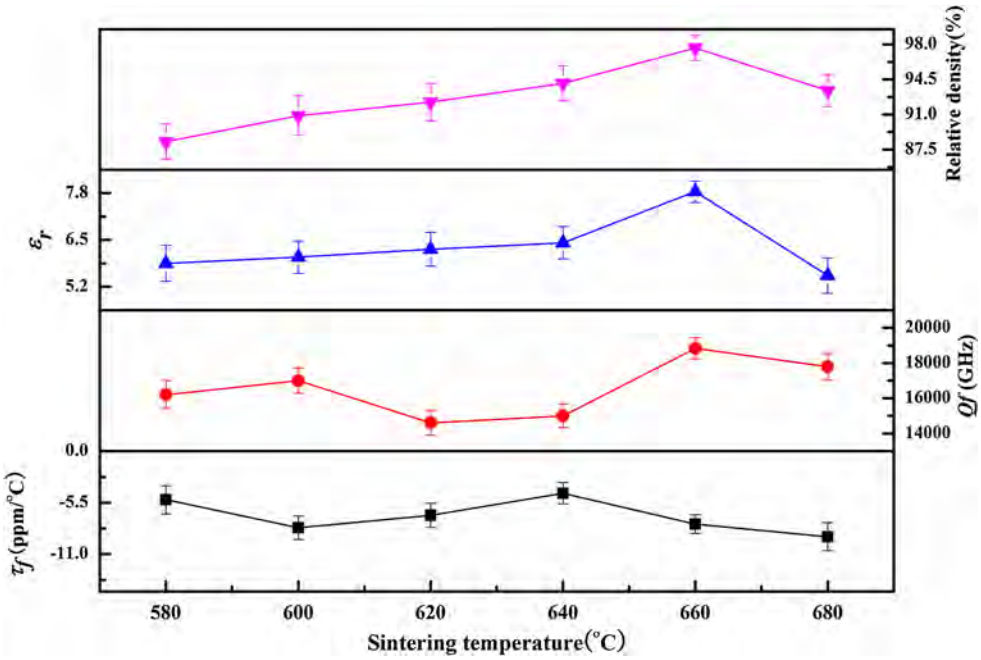

Fig. 5. Relative density and microwave dielectric properties (ε_r, $Q \times f$, and τ_f) of $Cu_3Mo_2O_9$ ceramic as functions of sintering temperature.

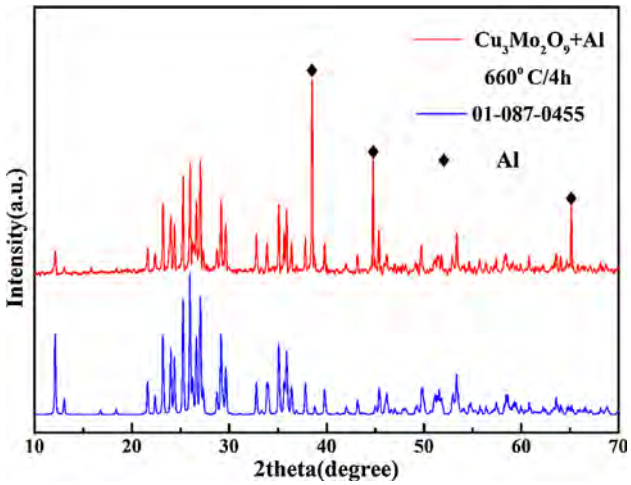

Fig. 6. XRD pattern of cofired $Cu_3Mo_2O_9$ ceramic with 20 wt.% aluminum.

obtained, remaining stable when sintered at temperatures from 580°C to 680°C.

Figure 4 shows SEM images recorded from polished and thermally etched surfaces of $Cu_3Mo_2O_9$ ceramic sintered at various temperatures. Obviously, all the samples exhibited uniform and dense microstructure with closely packed grain morphology and low degree of porosity. This result is in accordance with the high relative density of the sintered ceramics. Moreover, as the sintering temperature was increased beyond 640°C, the grain size increased significantly and abnormal grain growth and grain melting appeared.

Figure 5 shows the variation in the relative density and microwave dielectric properties (ε_r, $Q \times f$, and τ_f) of the $Cu_3Mo_2O_9$ ceramic as functions of sintering temperature. As shown in Fig. 5, the relative density showed a slight increase as the sintering temperature was increased from 580°C to 640°C, reaching a maximum value of $\sim 97.2\%$ at 660°C. The variation in the relative permittivity and quality factor exhibited a trend similar to that of density with relative maximum values ($\varepsilon_r \approx 7.2$, $Q \times f \approx 19{,}300$ GHz) obtained after sintering at 660°C. It is well known that microwave dielectric properties can be affected by many factors including intrinsic and the extrinsic factors such as densification, impurity, second phases, and crystal structure.[16,17] Thus, the decrease in relative permittivity (ε_r) and quality factor ($Q \times f$) can be attributed to porosity due to abnormal grain growth at elevated temperatures. On the other hand, the temperature coefficient of resonance frequency (τ_f) showed weak dependence on sintering temperature and fluctuated in the range from $-$ 4.5 ppm/°C to $-$ 9.1 ppm/°C. Note that the τ_f values are close to zero, which is beneficial for temperature stability. Generally, the sample sintered at 660°C exhibited the best microwave dielectric properties of $\varepsilon_r = 7.2$, $Q \times f = 19{,}300$ GHz, and $\tau_f = -7.8$ ppm/°C.

The influence of the porosity on the relative permittivity (ε_r) could be eliminated by applying Bosman and Having's correction[18,19]:

$$\varepsilon_{corr} = \varepsilon_r(1 + 1.5p),$$

where p is the fractional porosity, and $\varepsilon_{corrected}$ and ε_r are the corrected and measured values of permittivity, respectively. $\varepsilon_{corrected}$ is about 7.5 for the

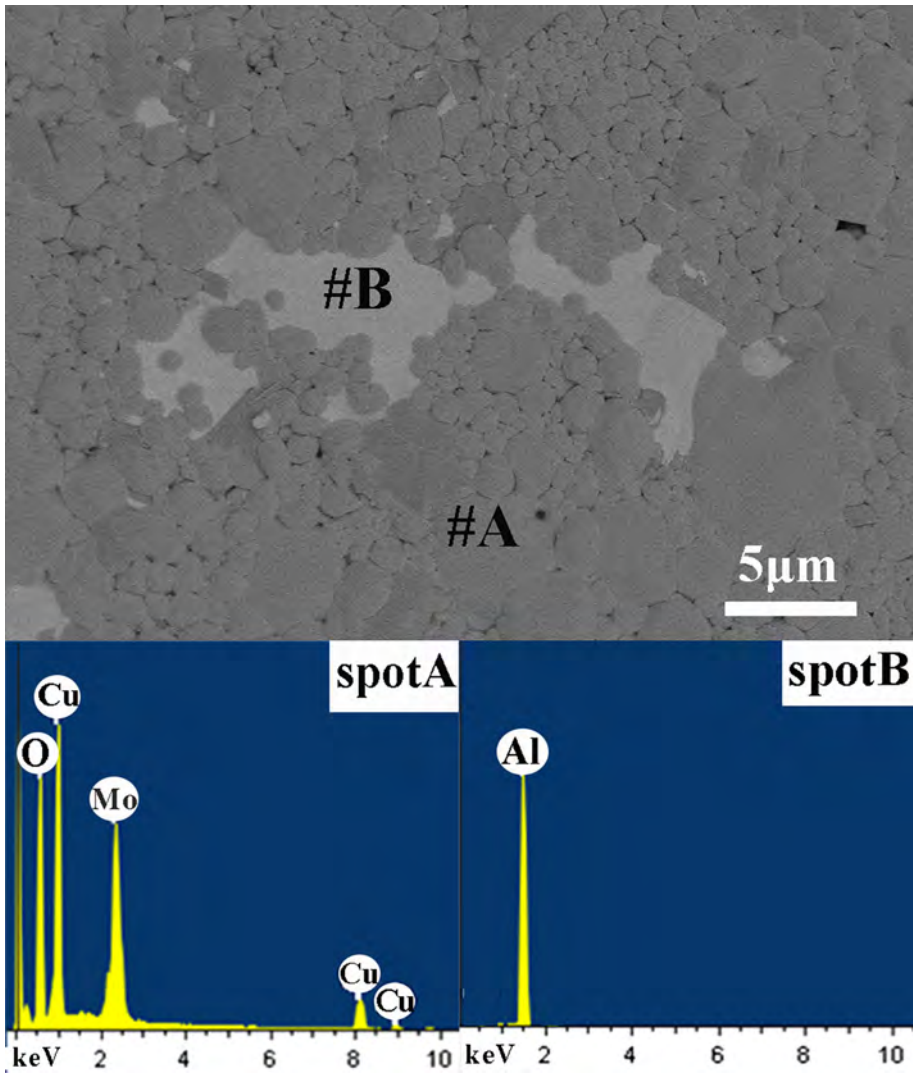

Fig. 7. Backscattered electron image micrograph and EDS analysis of cofired $Cu_3Mo_2O_9$ ceramic with 20 wt.% aluminum.

Table I. Comparison of microwave dielectric properties of some Mo-rich ceramics

Composition	S.T. (°C)	ε_r	$Q \times f$ (GHz)	τ_f (ppm/°C)	Ref.
Nd_2MoO_6	1350	13.8	66,400	− 53	26
$CaMoO_4$	1100	10.8	89,700	− 57	10
$BaNd_2(MoO_4)_4$	960	11.7	45,000	− 41	25
$BaSm_2(MoO_4)_4$	960	11.8	20,000	− 34	25
$BaCe_2(MoO_4)_4$	835	12.3	24,732	− 37	24
$Nd_2Mo_3O_{12}$	945	8.2	80,000	− 60	27
$La_2Mo_3O_{12}$	930	10.1	60,000	− 80	27
$(Na_{0.5}La_{0.5})MoO_4$	740	11.0	25,050	− 59	28
$(Na_{0.5}Nd_{0.5})MoO_4$	760	10.5	19,605	− 49	29
$(Na_{0.5}Ce_{0.5})MoO_4$	780	11.2	19,365	− 44	29
$Cu_3Mo_2O_9$	660	7.2	19,300	− 7.8	This work

$Cu_3Mo_2O_9$ sample sintered at 660°C, slightly larger than the measured value. Furthermore, the relative permittivity (ε_r) can be estimated as the sum of the ionic polarizability of individual ions (α_D^T) and molar volume (V_m) according to the Clausius–Mossotti equation[20,21]:

$$\varepsilon_r = \frac{1 + 2b\alpha_D^T/V_m}{1 - b\alpha_D^T/V_m},$$

where $b = 4\pi/3$. The sum polarizability of $Cu_3Mo_2O_9$ can be calculated using the additive rule:

$$\alpha_D^T = 3\alpha\left(Cu^{2+}\right) + 2\alpha\left(Mo^{6+}\right) + 9\alpha\left(O^{2-}\right).$$

The calculated theoretical permittivity of $Cu_3Mo_2O_9$ is 7.05. The relative error is about 0.3% for the measured value and 4.3% for the porosity-corrected value, indicating that that there is no other polarization mechanism operating in the $Cu_3Mo_2O_9$ ceramic in the microwave region beside ionic and electronic displacement polarization.[22,23]

Figure 6 illustrates the XRD patterns of the cofired $Cu_3Mo_2O_9$ ceramic with 20 wt.% aluminum sintered at 660°C for 4 h. The main peaks of $Cu_3Mo_2O_9$ and the characteristic peaks of Al (marked with dots) were both observed in the XRD patterns. The SEM image in Fig. 7 exhibits two kinds of grains with different morphology and elemental contrast. Combined with EDS analysis, the larger dark grains were determined to be aluminum element. These results confirm that the $Cu_3Mo_2O_9$ ceramic samples showed good chemical compatibility with Al when sintered at 660°C for 4 h.

Table I presents the microwave dielectric properties of some molybdate ceramics, most of which exhibit excellent microwave dielectric properties. By comparison, in spite of its inferior quality factor in contrast to $Ln_2Mo_3O_{12}$ (Ln = La, Nd) and $CaMoO_4$, $Cu_3Mo_2O_9$ ceramic showed the lowest sintering temperature (660°C), enabling its application in ultralow-temperature cofired ceramic (ULTCC) technology. Moreover, its near-zero temperature coefficient of resonant frequency (− 7.8 ppm/°C) guarantees the temperature stability of $Cu_3Mo_2O_9$ ceramic, which is superior to other molybdates.

CONCLUSIONS

An ultralow-temperature cofired $Cu_3Mo_2O_9$ ceramic in space group *Pnma* was prepared via a conventional solid-state reaction method. The phase purity, crystal structure, microstructure, and microwave dielectric properties were investigated using x-ray diffraction analysis, SEM, Raman spectroscopy, energy-dispersive spectrometry, and dielectric measurements. $Cu_3Mo_2O_9$ ceramic sintered at 660°C exhibited the highest relative density (~ 97.2%) and the best microwave dielectric properties with $\varepsilon_r = 7.2$, $Q \times f = 19{,}300$ GHz, and $\tau_f = -7.8$ ppm/°C as well as chemical compatibility with aluminum. All the results suggest $Cu_3Mo_2O_9$ as a good candidate for use in ultralow-temperature cofired ceramic technology.

ACKNOWLEDGEMENTS

This work was supported by the Natural Science Foundation of China (Nos. 21561008, 51502047, and 21761008), Natural Science Foundation of Guangxi Zhuang Autonomous Region (Nos. 2015GXNSFFA139003, 2016GXNSFBA380134, and 2016GXNSFAA380018), Project of Scientific Research and Technical Exploitation Program of Guilin (2016010702-2), Innovation Project of Guangxi Graduate Education (YCBZ2017052), and Project of Department of Science and Technology of Guangxi (2015AA07036).

REFERENCES

1. J. Varghese, S. Gopinath, and M.T. Sebastian, *Mater. Chem. Phys.* 137, 811 (2013).
2. J. Guo, D. Zhou, L. Wang, H. Wang, T. Shao, Z.M. Qi, and X. Yao, *Dalton Trans.* 42, 1483 (2013).
3. L.X. Pang, D. Zhou, Z.M. Qi, W.G. Liu, Z.X. Yue, and I.M. Reaney, *J. Mater. Chem. C* 5, 2695 (2017).
4. W. Li, L. Fang, Y.H. Sun, Y. Tang, J.W. Chen, and C.C. Li, *J. Electron. Mater.* 46, 1956 (2017).
5. N.M. Alford and S.J. Penn, *J. Appl. Phys.* 80, 5895 (1996).
6. D. Zhou, H. Wang, L.X. Pang, C.A. Randall, and X. Yao, *J. Am. Ceram. Soc.* 92, 2242 (2009).
7. G. Subodh, R. Ratheesh, M.V. Jacob, and M.T. Sebastian, *J. Mater. Res.* 23, 1551 (2008).
8. Y. Wang and R.Z. Zuo, *J. Eur. Ceram. Soc.* 36, 247 (2016).
9. J. Li, L. Fang, H. Luo, J. Khaliq, Y. Tang, and C.C. Li, *J. Eur. Ceram. Soc.* 36, 243 (2015).
10. G.K. Choi, J.R. Kim, H.Y. Sung, and H.K. Sun, *J. Eur. Ceram. Soc.* 27, 3063 (2007).
11. N. Joseph, J. Varghese, T. Siponkoski, M. Teirikangas, and M.T. Sebastian, *ACS. Sustain. Chem. Eng.* 4, 5632 (2016).
12. C.C. Li, H.C. Xiang, and L. Fang, *J. Electron. Mater.* 45, 262 (2016).
13. T. Hamasaki, H. Kuroe, T. Sekine, M. Hase, and H. Kitazawa, *J. Phys. Conf. Ser.* 150, 42 (2009).
14. V.N. Moiseenko, Y.I. Bogatirjov, A.M. Jeryemenko, and S.V. Akimov, *J. Raman Spectrosc.* 31, 539 (2000).
15. T. Sato, R. Kino, K. Aoki, H. Kuroe, and T. Sekine, *JPS. Conf. Proc.* 3, 014035 (2014).
16. E.S. Kim, B.S. Chun, R. Freer, and R.J. Cemik, *J. Eur. Ceram. Soc.* 30, 1731 (2010).
17. C.F. Tseng, *J. Eur. Ceram. Soc.* 35, 383 (2015).
18. A.J. Bosman and E.E. Havinga, *Phys. Rev.* 129, 1593 (1963).
19. D.W. Kim, I.T. Kim, B. Park, K.S. Hong, and J.H. Kim, *J. Mater. Res.* 16, 1465 (2001).
20. R.D. Shannon, *J. Appl. Phys.* 73, 348 (1993).
21. S.H. Yoon, D.W. Kim, S.Y. Cho, and H.K. Sun, *J. Eur. Ceram. Soc.* 26, 2051 (2006).
22. D. Zhou, C.A. Randall, L. Pang, H. Wang, and J. Guo, *J. Am. Ceram. Soc.* 94, 348 (2011).
23. R.D. Shannon, *J. Appl. Phys.* 73, 348 (1993).
24. N.K. James and R. Ratheesh, *J. Am. Ceram. Soc.* 93, 931 (2010).
25. D. Zhou, L.X. Pang, J. Guo, Y. Wu, G.Q. Zhang, W. Dai, H. Wang, and X. Yao, *J. Am. Ceram. Soc.* 94, 2800 (2011).
26. Y.C. Chen and M.Z. Weng, *J. Mater. Sci. Mater. Electron.* 26, 3502 (2015).
27. L.X. Pang, G.B. Sun, and D. Zhou, *J. Mater. Sci. Lett.* 65, 164 (2011).
28. H. Xi, D. Zhou, H. Xie, and W. Li, *Mater. Lett.* 142, 221 (2015).
29. H.H. Xi, D. Zhou, H.D. Xie, and W.B. Li, *Ceram. Int.* 41, 278 (2015).